

Supplementary Information:

The NH₃-SCR over Cu/SAPO-34 catalysts with various acid contents at low Cu loading

Tie Yu^a, Jun Wang^a, Meiqing Shen^{a, b*}, Wei Li^c

^a Key Laboratory for Green Chemical Technology of State Education Ministry,
School of Chemical Engineering & Technology, Tianjin University, Tianjin
300072, PR China

^b State Key Laboratory of Engines, Tianjin University, Tianjin 300072, PR China

^c General Motors Global Research and Development, Chemical Sciences and
Materials Systems Lab, 3500 Mound Road, Warren, MI 48090, USA

* Corresponding author: Meiqing Shen

Postal address:

School of Chemical Engineering and Technology, Tianjin University, 92 Weijin Road,
Nankai District, Tianjin 300072, China

Email: mqshen@tju.edu.cn

Tel./ Fax.: (+86) 22-27892301

XRD results

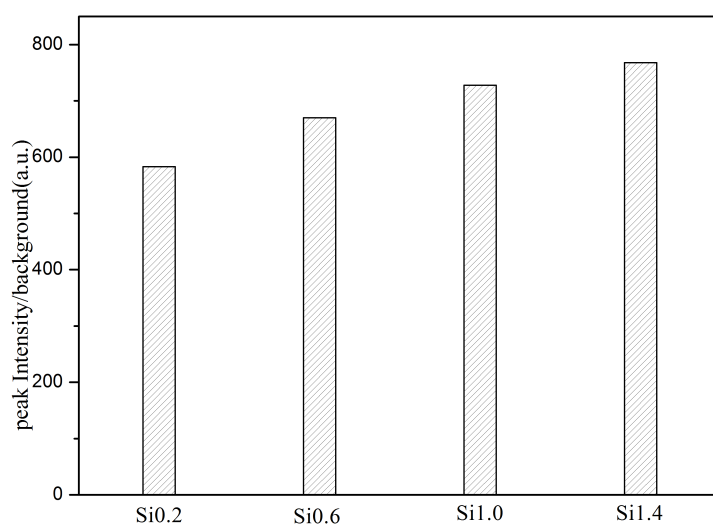


Fig. S1 the intensity of XRD profiles at 21.08° of SAPO-34 supports

The peak at 21.08° of SAPO-34 supports is usually used to compare the crystalline. And it is seen that the four SAPO-34 supports present the increasing crystalline with the increment of Si amounts.

NO oxidation

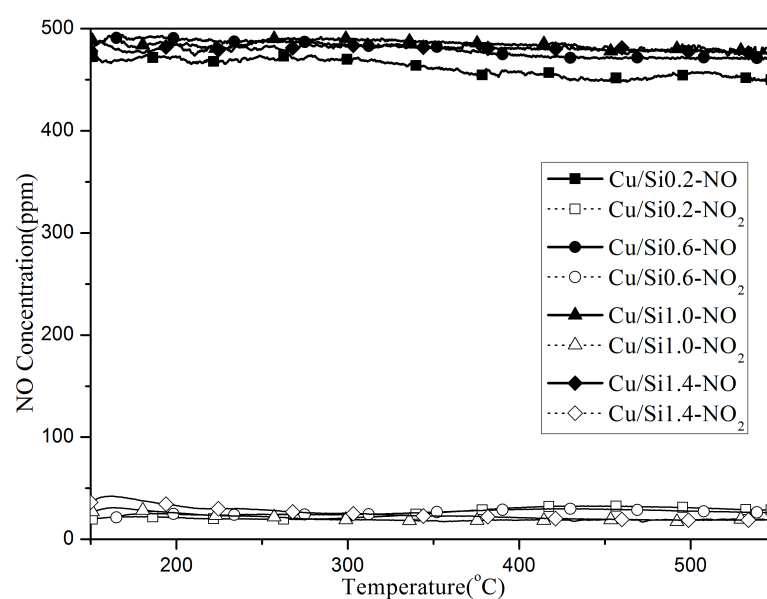


Fig. S2 the NO oxidation results over Cu/SAPO-34 catalysts. The conditions were: the inlets

consisted of 500 ppm NO, 5% O₂ with N₂ as the balance. The flow rate and the volume hourly

space velocity in all experiment were controlled at 500ml/min and 300,000h⁻¹.

The NO oxidation results over four Cu/SAPO-34 catalysts are listed in Fig. 2S.

During the whole temperature range, all catalysts show inferior activities and the NO

could hardly be oxidized.

EPR results

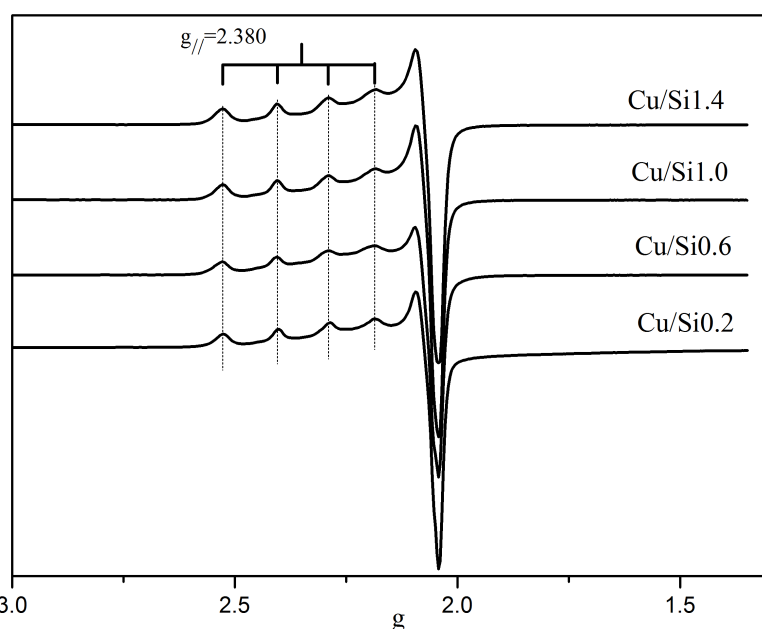


Fig. S3 the EPR spectra of Cu/SAPO-34 catalysts. Prior to the tests, the Cu/SAPO-34 catalysts

were vacuumed at 4.0×10^{-4} Pa for 1 hour at 120°C.

The EPR is inactive for CuO, binuclear species, or Cu⁺ ions but only active for isolated Cu²⁺ species [1]. So the EPR spectra can characterize the hyperfine structure of Cu²⁺ species. Fig. S3 shows that the four Cu/SAPO-34 catalysts contain only Cu²⁺ species in site (I) (Cu²⁺ (I)) [2, 3], displaced from the six-ring into the ellipsoidal cavity.

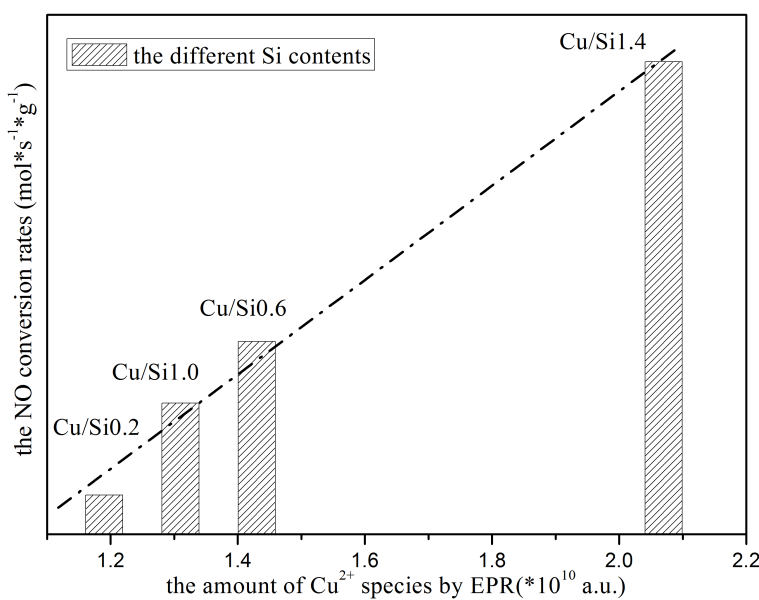


Fig. S4 the relation between the NO conversion rates and the Cu²⁺ contents over Cu/SAPO-34

catalysts. The Cu²⁺ contents were calculated by deconvolution of the EPR spectra.

The turnover frequency (TOF) is not calculated due to the semi-quantitation of Cu²⁺ contents by EPR. The intensity of EPR spectra is related to the Cu²⁺ contents, and the deconvolution of EPR spectra is used to represent the Cu²⁺ contents over catalysts¹. Fig. 4S conveys the TOF using the NO rates at 200 °C as a function of Cu²⁺ contents by EPR. It is seen that the TOF is a constant and the Cu²⁺ species are the active sites for NH₃-SCR over Cu/SAPO-34 [4].

NH₃-TPD

Fig. 3 presents that three are three acid sites for all of the zeolites, and Table 3 shows the sum of adsorbed NH₃ contents. In addition, the adsorbed NH₃ contents at different acid sites are listed in Table S1. It is seen that the strong acid sites for SAPO-34 and Cu/SAPO-34 increase with the raise of Si amounts.

The values of (Si+P)/Al can reflect whether the Si islands exist in SAPO-34 zeolites.

When the (Si+P)/Al is bigger than 1, the Si islands appear as the coordination structure of Si (n OAl, $n=0-3$). Nevertheless, the SAPO-34 zeolites do not contain Si islands when the the (Si+P)/Al is smaller than 1 [5]. The results of (Si+P)/Al for four SAPO-34 zeolites in Table S1 show that all of them contain less Si islands.

Table S1 the contents of desorbed NH₃ at various acid sites over zeolites

Sample	Weak acid sites(mmol/g)	Moderate acid sites(mmol/g)	Strong acid sites(mmol/g)	Sum(mmol /g)	(Si+P)/Al
Si0.2	0.020	0.084	0.093	0.197	1.17
Si0.6	0.028	0.093	0.149	0.270	1.27
Si1.0	0.021	0.126	0.151	0.298	1.35
Si1.4	0.033	0.137	0.165	0.335	1.38
Cu/Si0.2	0.007	0.028	0.040	0.075	/
Cu/Si0.6	0.007	0.092	0.096	0.195	/
Cu/Si1.0	0.020	0.075	0.107	0.202	/
Cu/Si1.4	0.027	0.088	0.128	0.243	/

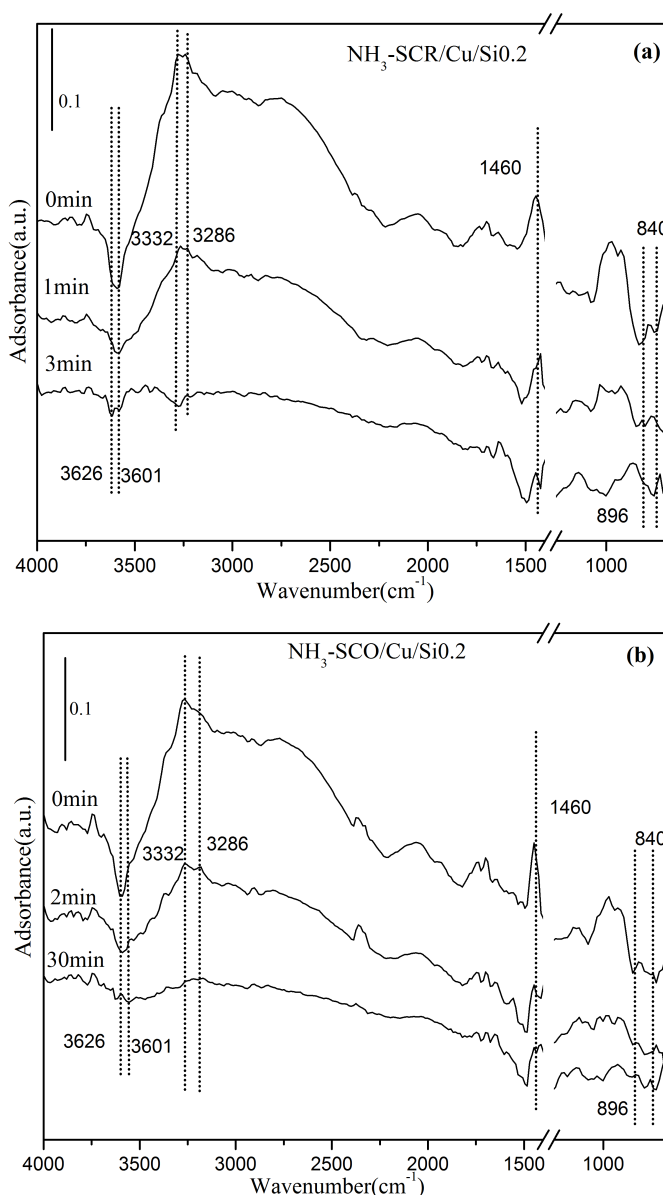
NH₃-SCR& NH₃ oxidation (SCO) at 410 °C(DRIFT)

Diffuse reflectance infrared Fourier transform spectra (DRIFTS) were carried on FT-IR spectrometer (Nicolet 6700) using a heatable environmental reaction cell with ZnSe windows, which was connected to a gas-dosing system. Prior to the experiments the samples were pretreated at 500 °C for an hour by 2% O₂ /He. The DRIFTS spectra were recorded from 4000 to 650 cm⁻¹ with a resolution of 2 cm⁻¹. Nicolet OMNIC software was used to process data.

The *in situ* DRIFTS were performed to research the influence of acid contents on NH₃-SCR/NH₃ oxidation, and the background spectra were collected before the samples were exposed to the absorbates. Firstly, The NH₃ chemisorption was

performed in 1% NH₃/He (500ppm) at 410 °C. A helium flow was used to purge the extra gas-phase NH₃ molecular after the saturation adsorption. Then, the samples were exposed to NO+O₂/O₂ for NH₃-SCR/NH₃ oxidation at 410 °C, respectively. The Cu/Si0.2 and Cu/Si1.4 were set as examples to explore the effect of acid contents on their different activities in NH₃-SCR/NH₃ oxidation.

The ascription of the acid sites can be seen in our previous work [6]. This study pays more attention on the NH₃ adsorbed on Brønsted acid sites.



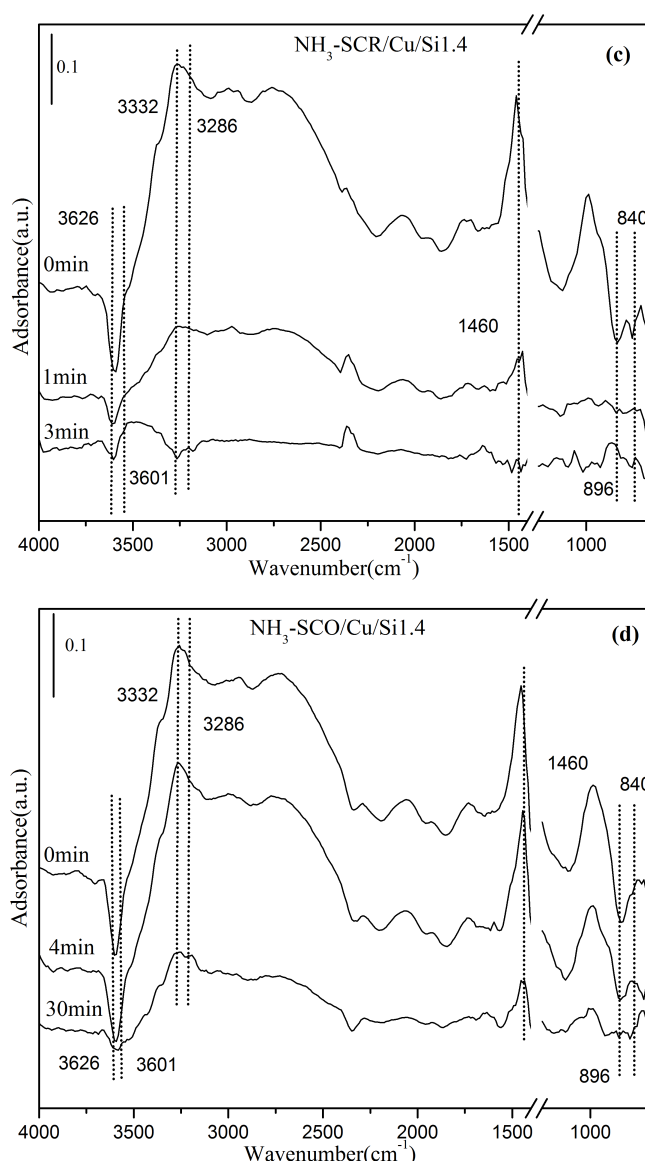


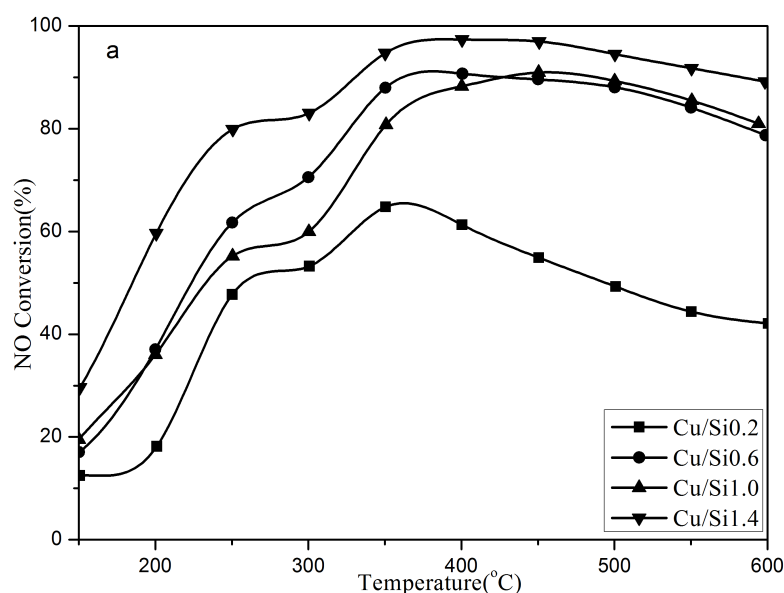
Fig. S5 DRIFTS spectra of NH₃-SCR/SCO over Cu/Si0.2 and Cu/Si1.4 catalysts at 410°C, units in Kubelka-Munk. (a) NH₃-SCR over Cu/Si0.2, (b) NH₃ oxidation over Cu/Si0.2, (c) NH₃-SCR over Cu/Si1.4, (d) NH₃ oxidation over Cu/Si1.4. The conditions: the NH₃ chemisorption was performed in 1% NH₃/He (500ppm) at 410 °C, then 500ppm NO and 30ml O₂ (2% vol)/He were cut in for (a) and (c); only 30ml O₂ (2% vol)/He were cut in for (b) and (d).

Firstly, the NH₃-SCR results in Fig. S5a and S5c show that the NH₃ species adsorbed on Brønsted acid sites perform more active in SCR reaction than that in NH₃ oxidation in Fig. S5b and S5d. The NH₃ species adsorbed on Brønsted acid sites take

much more times to participate in NH_3 oxidation. In addition, the Cu/Si1.4 shows more adsorbed NH_3 species than Cu/Si0.2 sample due to its high acid contents.

NH₃-SCR with H₂O and CO₂

The influence of H₂O and CO₂ to the NH₃-SCR activities is shown in Fig. S6. The NO conversions do not decline after the addition of H₂O and CO₂. Moreover, the H₂O and CO₂ in the feed inhibit the formation of by-products during SCR process. All of the results are consisted with our previous paper [6]. The positive reason of H₂O and CO₂ in the feed over Cu/SAPO-34 catalysts is investigated independently and the paper is conducted recently.



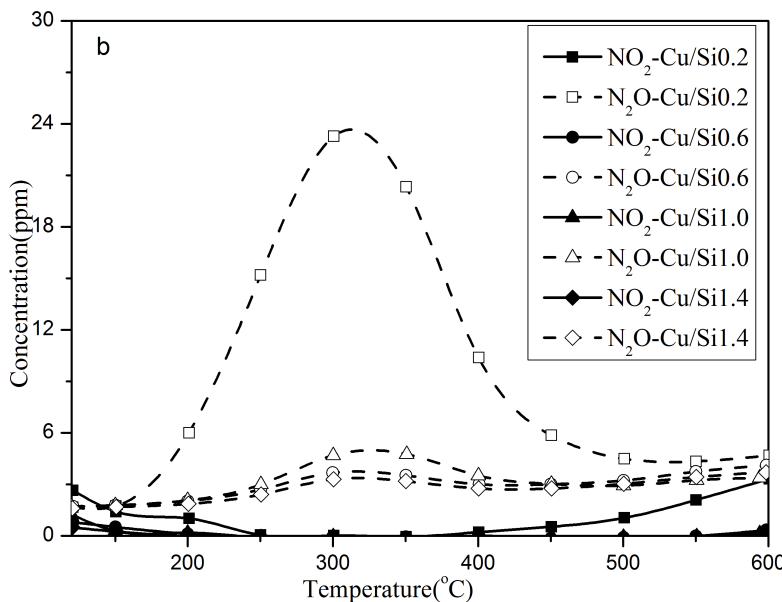


Fig. S6 the results of SCR activities over various Cu/SAPO-34 catalysts with H₂O and CO₂. (a)

the NO conversion; (b) the concentrations of NO₂、N₂O. The feed contains 500 ppm NH₃, 500 ppm NO, 5% O₂, 3% H₂O, 6% CO₂, N₂ is the balance. The flow rate and the volume hourly space velocity in all experiment were controlled at 500 ml/min and 300,000 h⁻¹

The ²⁹Si NMR results

The ²⁹Si MAS NMR (Nuclear Magnetic Resonance) experiments were performed on a Varian Infinity plus 300WB spectrometer at resonance frequencies of 70 MHz for ²⁹Si nuclei and the ²⁹Si MAS NMR spectra were recorded with a spinning rate of 5 kHz. Only the ²⁹Si NMR of Si0.2 and Si1.4 were used to investigate the influence of Si contents on the formation of Si islands in SAPO-34 molecular sieves.

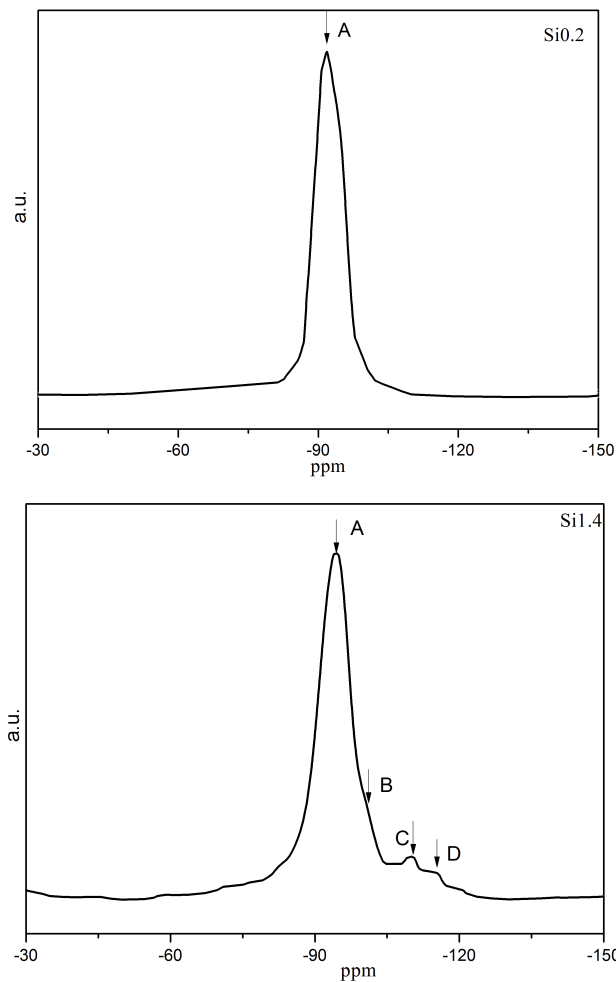


Fig. S7 the ^{29}Si NMR results of SAPO-34 supports

Our previous work [6] had presented that $(\text{Si}+\text{P})/\text{Al}$ can reflect the formation of Si islands in SAPO-34. If the mole ratio of the $(\text{Si} + \text{P})/\text{Al}$ is not bigger than 1, Si atom substitutes P and forms the $\text{Si}(\text{4OAl})$ species. If the ratio of $(\text{Si} + \text{P})/\text{Al}$ is bigger than 1, both the Si atom substitution P and Al occur and the Si islands $\text{Si}(\text{nOAl})$ ($n=0-3$) species exist. The results of $(\text{Si} + \text{P})/\text{Al}$ in Table S1 increase with the increment of Si contents. In addition, the NMR spectrum of Si0.2, in Fig. S7, shows only $\text{Si}(\text{4OAl})$ coordination structure (peak A), while the Si1.4 presents $\text{Si}(\text{4OAl})$ (peak A), $\text{Si}(\text{3OAl})$ (peak B), $\text{Si}(\text{1OAl})$ (peak C), and $\text{Si}(0\text{OAl})$ (peak D) species [6]. Consequently, it is concluded that the amounts of Si islands increase with the raise of

(Si + P)/Al over the four SAPO-34 zeolites.

H₂-TPR

Temperature Programmed Reduction (TPR) experiments were performed in a U-shaped tubular quartz reactor. Prior to reduction, the samples were first treated at 500 °C under a flow of 30 ml/min 2% O₂/N₂ and kept for 30 min. Then, the samples were cooled down to room temperature following by purging in N₂ with a flow of 30 ml/min. In the temperature programmed reduction process, the samples were heated to 900 °C at a ramping rate of 5 °C/min under a flow of 12 ml/min 5% H₂/N₂. The consumption of hydrogen was monitored by a thermal conductivity detector. The results are shown in Fig. S8.

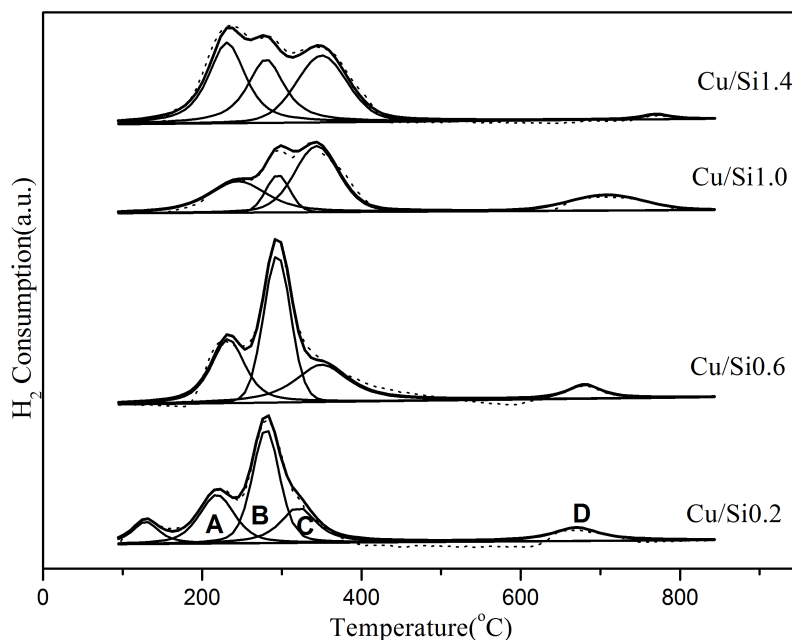


Fig. S8 H₂-TPR results of all Cu/SAPO-34 catalysts. The feed contained 5 vol.% H₂/N₂ and fed at a flow rate of 12cm³/ min and the experiment was performed from 30 °C to 900 °C with the heatingup rate of 5 °C /min.

In Fig. S8, the H₂ consumption peak from 200 °C to 600 °C can be divided into three peaks after deconvolution and curve stochastic fitting procedures by Lorentzian method, and the TPR curve of HSAPO-34 was subtracted as the baseline of the Cu/SAPO-34 sample. The peak at the lower temperature (peak A) represents the reduction of isolated Cu²⁺ to Cu⁺^[7-13], the moderate one (peak B) represents the reduction of the bulk Copper Oxide in zeolites from CuO to Cu⁰^[11, 13-14], and the third one (peak C) at the higher temperature comes from the reduction from Cu⁺ to Cu⁰^[7-13]. This H₂ consumption peak can be assigned to the reduction of “L (Low)-Cu⁺”, including the one obtained from the reduction of isolated Cu²⁺ and the original Cu⁺ existed on the framework of SAPO-34. Another H₂ consumption peak above 700 °C (peak D) can be attributed to the reduction of highly stable Cu⁺ to Cu⁰^[11-12, 15-16], which is named as “H (High)-Cu⁺”. Bulánek^[17] and Torre^[12, 13] found that the reducibility of Cu species in Cu-zeolites can be changed in a wide range by the coordination to zeolite framework oxygen. The more Al existed in the zeolites can cause higher negative charge of the zeolites, which strengthened the ligand of Cu species to the matrix. So the H₂ consumption peaks, reduction of Cu⁺ to Cu⁰ in Cu-zeolites, were above 600 °C. Richter^[16] found that the Cu⁺ species were reduced at 525 °C and 770 °C, and the H₂ consumption at the higher temperature was due to the formation of stable Cu⁺ species on Cu-zeolites. It is deduced that the H (High)-Cu⁺ coordinated to framework oxygen is more stable and more difficult to be reduced for the higher negative charge of zeolites. Moreover, the Cu/Si0.2 exhibits peaks at 130 °C, which are due to the reduction of surface CuO cluster to Cu⁰^[9, 10, 12],

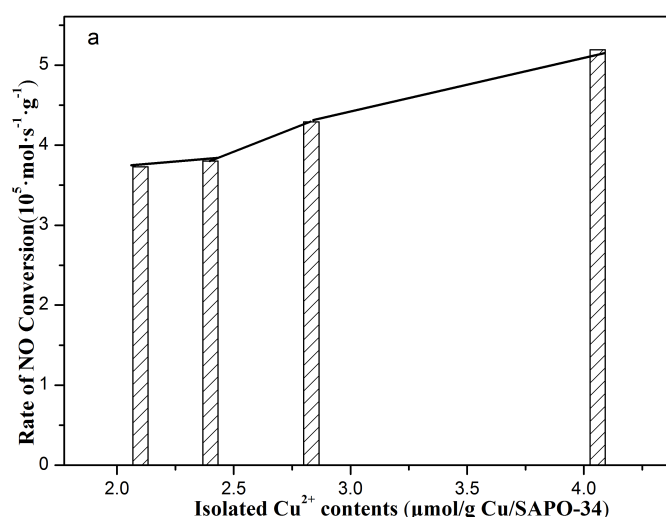
^{13, 16]}. Moreover, it is seen that the support has great impact on Cu species over the four Cu/SAPO-34 samples in Table S2. The influence of acid contents on the various Cu species by ion-exchange method had been discussed in the previous work ^[6].

Table S2 the contents of different Cu species on Cu/SAPO-34 from the H₂-TPR results

Sample	Copper Species Content ($\mu\text{mol/g}$ Cu/SAPO-34)				
	Surface CuO Cluster	Isolated Cu ²⁺	Bulk Copper Oxide in Cage	Cu ⁺	Amount
Cu/Si0.2	0.425	2.171	1.793	0.566	4.956
Cu/Si0.6	0	2.832	2.124	0.661	5.616
Cu/Si1.0	0	2.360	0.472	2.171	5.002
Cu/Si1.4	0	4.059	1.652	0	5.616

Explanation: The H₂-TPR of CuO is used to get the semi-quantitative assessment of different Cu species in Cu/SAPO-34. Especially, the Cu⁺ contents are calculated as follows: Amount of Cu⁺= [H₂ consumption_(peak C)+ H₂ consumption_(peak D)- H₂ consumption_(peak A)]

In addition, the main difference of this work is to further study the influence of acid contents on the SCR activity of Cu/SAPO-34, so the sample system is well designed. The Cu loading is controlled at low level to stress the role of acid content. And the following results in Fig. S9 show that none of the Cu species presents the direct relation with NO conversion as that with acid content in Fig. 6.



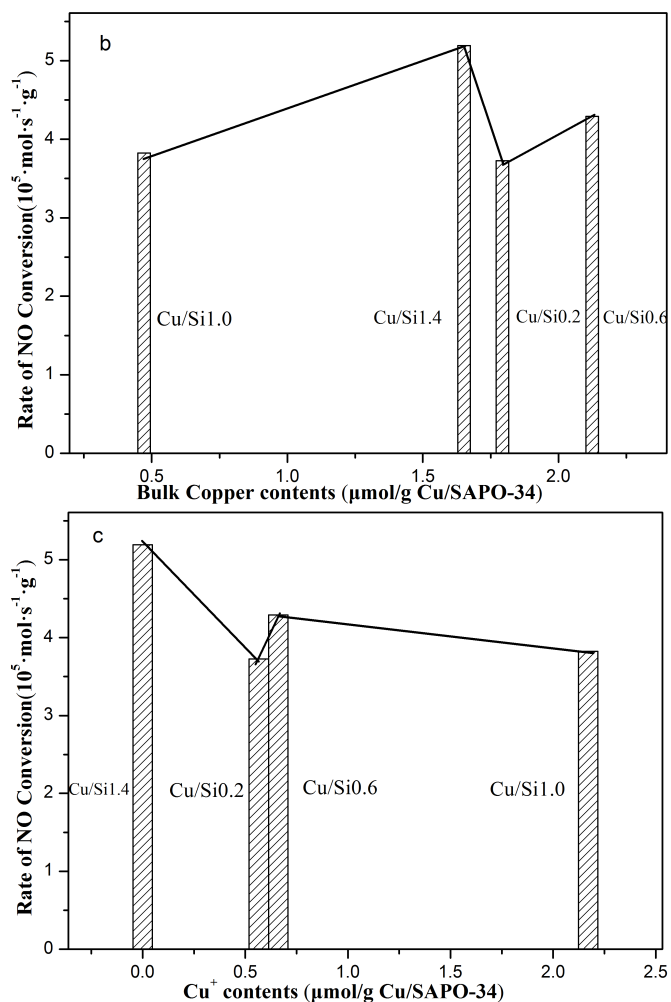


Fig. S9 the correlation of rate of NO conversion on Cu/SAPO-34 samples at 250 °C with respect to (a) Isolated Cu^{2+} contents; (b) Bulk Copper Oxide contents; (c) Cu^+ contents.

Reference

- [1] A. V. Kucherov, C. P. Hubbard, T. N. Kucherova, M. Shelef, *Appl. Catal., B*, 1996, 7, 285.
- [2] M. Zamadics, X. Chen, L. Kevan, *J. Phys. Chem.*, 1992, 96, 2652.
- [3] M. Zamadics, X. Chen, L. Kevan, *J. Phys. Chem.*, 1992, 96, 5488.
- [4] J. Xue, X. Wang, G. Qi, J. Wang, M. Shen, W. Li, *J. Catal.*, 2013, 297, 56.
- [5] L. Xu, A. Du, Y. Wei, Y. Wang, Z. Yu, Y. He, X. Zhang, Z. Liu, *Microporous Mesoporous Mater.*, 2008, 115, 332.

- [6] J. Wang, T. Yu, X. Wang, G. Qi, J. Xue, M. Shen, W. Li, *Appl. Catal., B*, 2012, 127, 137.
- [7] A. Sultana, T. Nanba, M. Haneda, M. Sasaki, H. Hamada, *Appl. Catal., B*, 2010, 101, 61-67.
- [8] Y. Wan, J. Ma, Z. Wang, W. Zhou, S. Kaliaguine, *J. Catal.*, 2004, 227, 242-252.
- [9] J.Y. Yan, G.D. Lei, W.M.H. Sachtler, H.H. Kung, *J. Catal.*, 1996, 161, 43-54.
- [10] J.Y. Yan, W.M.H. Sachtler, H.H. Kung, *Catal. Today*, 1997, 33, 279-290.
- [11] M. Richter, M.J.G. Fait, R. Eckelt, *Appl. Catal. B*, 2007, 73, 269-281.
- [12] C. Torre-Abreu, M.F. Ribeiro, C. Henriques, G. Delahay, *Appl. Catal. B*, 1997, 12, 249-262.
- [13] C. Torre-Abreu, M.F. Ribeiro, C. Henriques, G. Delahay, *Appl. Catal. B*, 1997, 14, 261-272.
- [14] R. Kefirov, A. Penkova, K. Hadjiivanov, S. Dzwigaj, M. Che, *Micropor. Mesopor. Mater.*, 2008, 116, 180-187.
- [15] D. Berthomieu, G. Delahay, *Catal. Rev.*, 2006, 48, 269-313.
- [16] M. Richter, M.J.G. Fait, R. Eckelt, M. Schneider, J. Radnik, D. Heidemann, R. Fricke, *J. Catal.*, 2007, 245, 11-24.
- [17] R. Bulánek, B. Wichterlová, Z. Sobalík, J. Tichy, *Appl. Catal. B*, 2001, 31 , 13-25.